Dead time of an anger camera in dual-energy-window-acquisition mode

Kenneth R. Zasadny, Kenneth F. Koral, and Fayez M. Swailem[a)]
Internal Medicine, Division of Nuclear Medicine, The University of Michigan Medical Center, Ann Arbor, Michigan

(Received 9 July 1992; accepted for publication 8 January 1993)

Two side-by-side energy windows are sometimes employed in quantitative single photon emission computed tomography (SPECT) studies. The count-rate losses at high activities for a GE400AT camera were measured in such a dual-window-acquisition mode by imaging a decaying source composed of a hot sphere within a warm cylinder. The data in each window was either kept separate or combined for purposes of dead-time correction and the paralyzable model was assumed. In addition, correction factors were derived from a "monitor" source at the edge of the camera. Finally, energy spectra for only the monitor-source region of interest and for the entire camera were obtained under both low- and high-count conditions and compared. With ^{99m}Tc (1) the spectral measurements show no peak shift but reveal pulse-pileup spectral degradation. (2) The monitor-source corrections do not agree well with those from the model, presumably because of the differential effects of such degradation. For this camera the preferred correction method for patients is one using the model and two, effective, phantom-derived dead times for the separate data from the two windows. The two effective dead times are needed to compensate for pulse pileup adding more counts to the lower-energy window than to the higher-energy one at high rates. For ^{99m}Tc, the effective dead time to correct data in the 93–123 keV window is 7.0 ± 0.14 μs and for that in the 124–154 keV window 5.95 ± 0.10 μs, and for ^{131}I, for data in the 260–332 keV window 18.8 μs and for that in the 333–405 keV window 14.3 μs.

I. INTRODUCTION

Anger-camera dual-energy-window-acquisition mode is utilized for the purpose of correcting for Compton scattering within patients. From the lower-energy window, one derives an estimate of the number of scattered gamma rays that are included within the higher-energy window. This value can then be subtracted from the counts in that window.[1] An example of the application is quantification of absolute activity in patients that have received a therapy dose of a ^{131}I-labeled monoclonal antibody.[2,3] Imaging therapy patients after the administration of a large amount of radioactivity can lead to significant losses of counts in the resulting images.[2]

Previous efforts[4–12] have modeled the dead-time behavior of anger cameras for radioisotopes with a single energy window at high-counting rates. Camera dead time has been shown to be dependent on the scattering condition in the source. The reason is that count rates from a single photopeak window do not account for lower-energy scattered photons, which do contribute significantly to the dead time of the camera electronics. Two studies[13,14] have commented on the difference between corrections based on a model and those based on a monitor source.[15] For ^{131}I with a single photopeak window using a GE400AT, the latter[14] implies that the monitor-source method gives accurate corrections only for regions in the field of view that are in close proximity to the monitor source.

We measured the dead-time losses of a GE400AT anger camera in dual-energy-window-acquisition mode for clinical situations where dead-time losses are at a fairly low level ($\leqslant 25\%$). Our particular version of this camera has a 1/2-in.-thick crystal since it is used extensively for ^{131}I imaging. We investigated ^{99m}Tc, for its own interest and also for guidance in choosing a method for counting-loss adjustment for ^{131}I. To test the reliability of the monitor-source method, we compared the dead-time correction factors from this method to those from a paralyzable-model fit to decaying-source data. The latter should have good accuracy, at least for the phantom used to establish the dead-time constant, and so can provide the check on the monitor-source method. To determine whether to handle the data from each window separately or to combine the data for purposes of dead-time correction, we investigated both of these possibilities. In a reduced study guided by the ^{99m}Tc results, we studied a ^{131}I-labeled agent.

II. THEORY

The dead-time correction factor C can be defined to correct the observed count rate N', to produce an estimate of the true count rate N.

$$N = CN'. \tag{1}$$

Here, the observed count rate is that found in the image recorded by the computer attached to the gamma camera.

To obtain the dead-time correction C, one method, pioneered by Freeman,[15] observes the counting losses from a "monitor source." One obtains the true monitor-source count rate N_{ms}, by measuring its count rate alone. Then, one defines a monitor-source dead-time-correction factor C_{ms} as simply

$$C_{ms} = \frac{N_{ms}}{N'_{ms}}, \tag{2}$$

where N'_{ms} is the monitor-source rate when the object of interest is being imaged. The monitor-source rates are obtained by drawing a region of interest about that source in

 0094-2405/93/20(4)/1115/6/$1.20

an image, applying it to all successive images, and taking into account the duration of each image acquisition. Also, each N'_{ms} is corrected for decay back to the time of the image that yielded N_{ms}. Note that the method assumes there is neither spatial distortion nor spectral degradation with increased count rates.

Since previous investigators[5] have shown the behavior of the GE400AT camera to closely approximate the paralyzable dead-time model, we have chosen to use it as our second method. In this model

$$N' = Ne^{-N\tau}, \tag{3}$$

where τ is the dead-time constant. With this model, it can easily be shown[16] that for a decaying source which has a disintegration constant λ, and which is measured at time t, $\lambda t + \ln N'$ can be plotted against $e^{-\lambda t}$ and τ can be related to the slope and intercept of the best fit to that data by

$$\tau = -(\text{slope})e^{-\text{intercept}}. \tag{4}$$

The relationship [from Eqs. (1) and (3)] between the observed count rate N' and the paralyzable-model dead-time correction factor C_p is

$$C_p = e^{N'\tau C_p}. \tag{5}$$

One can solve for C_p for a given N' and τ by iteration. That is, one guesses a C_p and then checks if it is consistent with Eq. (5) for the given N' and τ. If not, it is varied until the equation is satisfied.

III. METHODS

A cylindrical water-filled phantom of 22 cm height $\times$ 20 cm diam containing an off-axis 6-cm-diam sphere was used to approximate the scattering conditions that would be encountered for imaging a tumor in a patient. Four separate experiments were performed. In experiments 1 and 2, both the cylinder and sphere contained ^{99m}Tc activity, with the sphere containing a 7:1 activity concentration ratio compared to the surrounding cylinder background activity concentration. In experiment 3, a cylinder containing 962 MBq of ^{99m}Tc without a sphere was tested. In experiment 4, ^{131}I was used in the same proportions as in experiments 1 and 2.

Experiment 1. In experiment 1, the dead-time correction factor was determined from a monitor source and from the decaying source method with the camera at four angles relative to the phantom. Energy windows were 93–123 keV for measurement of scatter and 124–154 keV for the photopeak. The camera was positioned at 0°, 90°, 180°, and 270° relative to the axis running from cylinder "center" to sphere center. The sphere was 5.7 cm off-axis and nearest the camera at 0°. The monitor source was constructed by placing 7.4 MBq of ^{99m}Tc activity on a 2.5 cm circle cut from a silica-gel-impregnated glass-fiber sheet (Gelman Sciences Inc. ITLC SG, Product No. 61886, Ann Arbor, Michigan) and sealing with tape. It was placed on the surface of the camera collimator off to the side and out of the view of the cylindrical phantom. The monitor source was covered with 0.64 cm of lead to prevent photons from the phantom entering the monitor-source region of interest.

Ten measurements of the monitor source plus phantom were taken over a 20 h time period. Measurement times were selected so that the parameter $e^{-\lambda t}$ was evenly distributed; also, acquisition times were adjusted at later counting times so that all data would have similar counting statistics. The count rate for the monitor source alone was measured both before and after the phantom-plus-monitor-source experiment as a check on camera stability.

Experiment 2. Experiment 2 was performed 2 months after experiment 1. Except for slight variations in the activity levels, the phantom for experiment 2 was identical to that for experiment 1. Data were taken at 0° with the scatter window lower-energy level at 93, 97, 101, 105, and 109 keV.

Experiment 3. This experiment looked for spectral changes at specific camera-face locations at high-count rates. A special, Macintosh-based acquisition system[17] was used to make this possible. The spectrum within the monitor-source region of interest alone and that for the entire camera face were obtained at high and low camera count rates. First, the monitor source alone was placed on the camera and an energy spectrum for its region of interest (RoI) obtained (whole-camera count rate for the sum of the direct and scatter windows was about 1 Kcps). Then the cylindrical source was placed within the camera field of view. Another spectrum in the monitor-source RoI and one for the entire camera face were obtained (rate defined above now about 40 Kcps). Finally, three half-lives were allowed to elapse without moving the sources and a final spectrum for the entire camera face was obtained (rate defined above now about 5 Kcps).

Experiment 4. In experiment 4, a total of 740 MBq of ^{131}I was placed in the cylinder/sphere phantom. The main window was set symmetrically about the photopeak and the scatter window was the same size, with the nominal values being 333 to 405 and 260 to 332 KeV. Eight measurements were taken with the camera at 0° over a 14 day period. Measurement times were determined so that the parameter $e^{-\lambda t}$ was relatively evenly distributed. No monitor source was employed. Great care was taken so the experimental conditions were duplicated during each measurement period. Acquisition times were again extended for later time points.

IV. RESULTS

Dead-time constants for ^{99m}Tc. Data from experiments 1 and 2 were analyzed by linear least-squares fitting to the paralyzable dead-time model. Results were determined for (1) the photopeak-window count rate, (2) the scatter-window count rate, and (3) the sum of count rates for both windows (combined window). Excellent fits were obtained for all three, with the correlation value equal to 0.998 or better. Table I shows the resulting paralyzable dead-time constant τ, as a function of the experimental conditions. The results at 0° on 5/13 are comparable to those from 7/15. On 5/13 there appears to be no correlation between

TABLE I. Dead-time constant for paralyzable model with two ways of analyzing data. Windows-Scatter: 93–123 KEV. Photopeak: 124–154 KEV. (Mean ±1 standard deviation 7.00±0.14, 5.95±0.10, 3.35 ±0.05.)

		Dead time constant, τ (microseconds)		
		Way 1		Way 2
Date	Angle	Scatter	Photopeak	Combined
5/13	0°	6.97	5.93	3.33
	90°	6.80	5.87	3.29
	180°	7.02	5.83	3.30
	270°	7.17	6.00	3.39
7/15	0°	7.05	6.09	3.41

TABLE III. Fraction of counts within the scatter window as a function of observed combined count rate.

	^{99m}Tc		^{131}I
Rate	Scatter-to-total fraction	Rate	Scatter-to-total fraction
4.3 Kcps	0.360	15.4 Kcps	0.376
7.2	0.360	18.9	0.380
13.2	0.360	23.6	0.382
17.0	0.361	27.0	0.386
20.4	0.362	30.4	0.388
24.8	0.364	34.0	0.393
28.9	0.367	35.4	0.397
32.0	0.368	37.4	0.399
35.4	0.370		
38.5	0.371		

the dead-time constants and the slight variation in scattering conditions at the different camera angles. That is, scattering conditions are the same at camera angles 90° and 270° and the variation in τ is as great between these cases as between any other two cases. The slight changes in experimental condition are, therefore, declared negligible within experimental error and all five τ values considered samples of the same variable. The average of the five dead-time values for ^{99m}Tc is 7.00±0.14, 5.95±0.10, and 3.35 ±0.05 μs for data in the scatter(93–123 keV), photopeak(124–154 keV), and combined windows, respectively (mean ± standard deviation).

Table II shows the dead-time correction factors C_p, that are calculated from these dead times at an observed combined count rate of 35 Kcps. We will argue in the discussion that keeping the data separate is preferred. Since C_p is a multiplicative factor, the error produced in the scatter correction by using one method when another is right can be found easily. For example, if the data are combined for the purpose of dead-time correction when separate is right, an error of $(1.14-1.11)/1.11=2.7\%$ is made in the corrected scatter-window count rate for ^{99m}Tc at a combined-window rate of 35 Kcps.

Scatter-to-total fraction. For the camera as a whole, we also calculated the ratio of the counts in the scatter window over the total counts in both windows, as a function of observed combined count rate. For all tests in all experiments, this fraction increased as the count rate increased, presumably due to spectral changes. The trend is shown in Table III for a typical ^{99m}Tc experiment and also for the ^{131}I measurement. This increase of count fraction within the scatter window is consistent with the lower dead-time correction factor for the scatter window compared to the direct window (Table II) and means that our reported dead times are effective values that also compensate for spectral distortions.

TABLE II. Dead-time correction factors as a function of combining or keeping windows separate. Combined count rate[a]=35 Kcps.

	^{99m}Tc	^{131}I
Scatter window Data separate	1.11	1.47
Direct window Data separate	1.17	1.63
Data combined	1.14	1.57

[a]Combined count rate=sum of scatter-window rate plus photopeak-window rate.

Monitor source. Figures 1(a)–1(c) show the model correction factor C_p, and the factor determined from the monitor source C_{ms}, as a function of observed camera count rate. For the data from the scatter-window [Fig. 1(a)], there is poor agreement between the dead-time correction factor determined from the monitor source and that derived from the dead-time model especially at the higher-count rates. The camera rotation angle does not have an effect. The correction factor derived from the monitor source does not even seem to depend on the observed counting rate at the higher rates. Raising the lower-energy threshold for the scatter window up to 109 keV (not shown) did not improve the agreement. It is concluded that the monitor-source correction factors for the scatter-window data are heavily distorted from the values for the camera as a whole. For the direct-window and combined-window data [Figs. 1(b) and 1(c)], the monitor-source correction factors rise faster than those for the dead-time model. We feel that, because the monitor-source region of interest has a different spectrum than that in the region of interest for the whole camera and because spectral degradation is occurring (see below), the monitor-source correction factors are not appropriate for the whole camera. We conclude that the model-dependent approach is preferable.

The monitor-source method was not investigated with ^{131}I since the monitor-source and whole-camera spectra are again different. The measurements reported in Table II indeed indicate that spectral distortion does occur with ^{131}I. However, we have not explicitly shown that results from the monitor-source-method disagree with those from the model for ^{131}I.

Spectral distortion. Figures 2(a) and 2(b) compare the whole-camera spectrum under low- and high-count conditions. The location of the peak is unshifted but the valley at channel 560 tends to get filled in, presumably due to pulse pileup. The high-energy tail above the photopeak shows that pulse pileups are indeed not all being rejected. The ratio of the counts in the scatter window over total counts

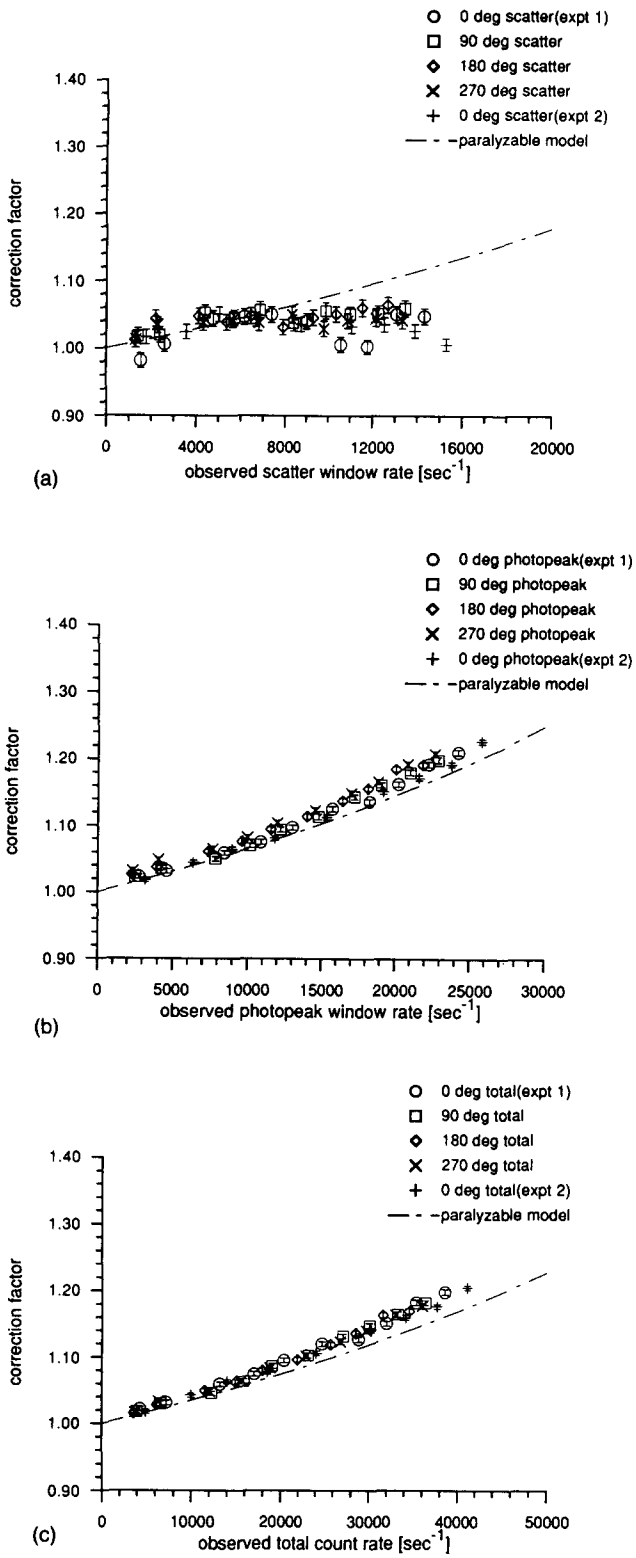

FIG. 1. Plots of the ^{99m}Tc dead-time correction factor vs the observed count rate in the window specified: (a) scatter window, (b) photopeak window, and (c) sum of both windows. Symbols refer to results from the monitor-source method. The dashed lines give the predictions from the paralyzable model.

in both windows goes up from 36.15% to 36.60%. Figures 2(c) and 2(d) make the same comparison for the monitor-source spectrum. Here changes are not as apparent but the ratio of the counts in the scatter window over total counts in both windows goes up from 8.20% to 8.69% indicating that spectral degradation is occurring.

Dead-time constants for ^{131}I. For the ^{131}I phantom of experiment 4, linear least-squares fitting of Eq. (7) to the scatter-window (r=0.981), photopeak-window (r=0.989), and combined-window (r=0.987) data was performed. The effective dead-time constant was 18.8, 14.3, and 8.24 μs for the scatter, photopeak, and combined data, respectively. It was to be expected that the constant for a given count rate in a particular energy window might be different for the ^{131}I radioisotope compared to ^{99m}Tc for a number of reasons. First, the energy spectrum is different, since it depends on the photon emissions. Second, the time it takes for the camera electronics to process a higher-energy (hence higher pulse height) signal is expected to be extended. Thus, the different and longer τ values seem reasonable.

Table II shows that keeping the data separate for separate windows is even more important for ^{131}I than for ^{99m}Tc.

IV. DISCUSSION

In the simplest conception of the operation of a gamma camera, one thinks of the shape of the spectrum remaining the same as the count rate changes. Then the number of counts within a given energy window as a fraction of all counts does not change either. In fact, for the camera as a whole, we have seen that the counts in the scatter window, as a fraction of the total counts in both windows, increase with count rate for all our experiments. We have also seen that pulse pileup is occurring, and it presumably is the cause of the spectral distortions at higher rates both with ^{99m}Tc and with ^{131}I.

A patient will have a spectrum similar to that from the cylindrical phantom. Since spectral degradation will similarly relieve the need for as much dead-time correction for the data in the scatter window relative to that in the direct window, it is more accurate to employ two effective dead-time correction factors derived from separate effective dead times with the model method. To employ only one "average" dead time, that derived by combining the data, would overcorrect the data in the scatter window and undercorrect that in the direct window.

Considering the monitor-source correction compared to the model correction, there is disagreement at high-count rates with ^{99m}Tc. For the data in the scatter window considered by itself the monitor source predicts a lower dead-time correction factor than does the model; this disagreement can be explained by pileup moving relatively larger numbers of counts into the monitor-source scatter window than into the whole-camera scatter window. For the data in the direct window considered alone, the monitor source predicts a slightly higher dead-time correction than the model. This presumably occurs because more counts move into the window for the whole-camera spectrum than for the monitor spectrum alone. This explanation is plausible because the whole-camera spectrum has many more scatter counts just below the low-energy edge of the direct window. The result for the combined data where the monitor-

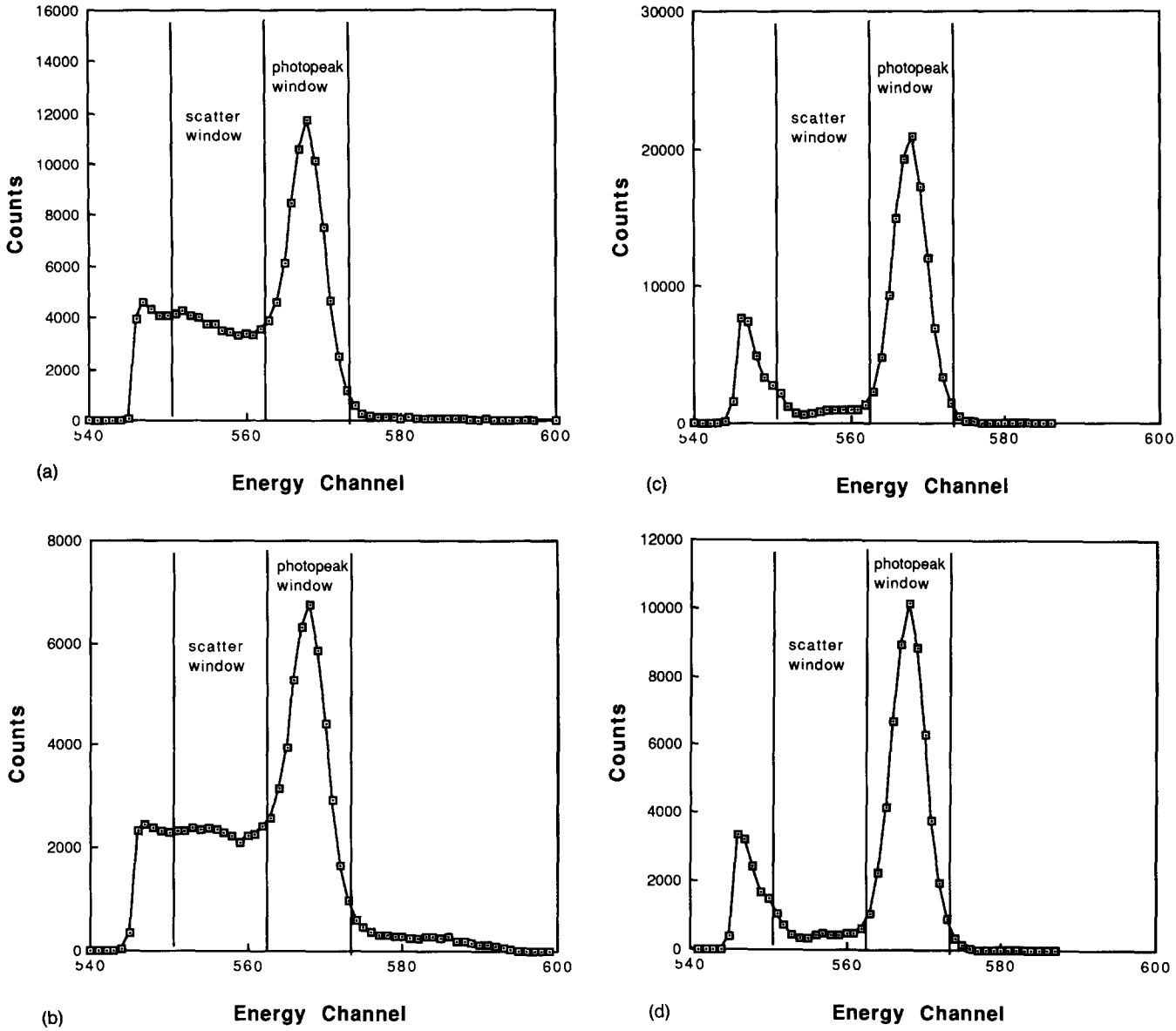

FIG. 2. Plots of ^{99m}Tc energy spectra with an extended object and monitor source in the field of view. The locations of both the photopeak and the scatter window are indicated: (a) is for the camera as a whole when the count rate is low; (b) is the same when the rate is high; (c) is for a region of interest over the monitor source when the rate is low; (d) is the same when the rate is high.

source correction is again larger than that from the model is presumably due to the same sort of effect.

Finally, we note that the accuracy of the monitor-source method for a different camera may be different than in the results we have observed. However, our experience indicates that the use of a monitor source should be validated for any given camera.

V. CONCLUSIONS

Although the use of a monitor source to measure counting losses from an anger camera seems attractive, results of this work for ^{99m}Tc show that in the dual-energy-window-acquisition mode, dead-time correction factors derived from a monitor source are somewhat unreliable for the main object with a GE400AT camera. It is recommended that for quantitative imaging of tumor activity in a patient with this camera, one should derive a separate correction factor for each window based on the value of the paralyzable dead time measured for a phantom. These dead times are 7.0 ± 0.14 μs for a scatter window (93–123 keV) and 5.95 ± 0.10 μs for a direct window (124–154 keV) with ^{99m}Tc and 18.8 μs (260–332 keV) and 14.3 μs (333–405 keV) for ^{131}I with the 1.27-cm-thick-crystal GE400AT.

We are aware that a patient with a different activity distribution would not be fit exactly by the model with these constants but we think the model-method is safer than the monitor-source method. If someone does desire to use a monitor source, then the data from the two windows should probably be combined to avoid a large error for the scatter-window data.

[a]New affiliation: Nuclear Medicine, Veterans Administration Medical Center, Tucson, Arizona.

[1]K. F. Koral, F. M. Swailem, S. Buchbinder, N. H. Clinthorne, W. L.

Rogers, and B. M. W. Tsui, "SPECT dual-energy-window Compton correction: Scatter multiplier required for quantification," J. Nucl. Med. **31**, 90–98 (1990).

[2]K. F. Koral, K. R. Zasadny, F. M. Swailem, S. F. Buchbinder, I. R. Francis, M. S. Kaminski, and R. L. Wahl, "Importance of intratherapy single-photon emission tomographic imaging in calculating tumor dosimetry for a lymphoma patient," Eur. J. Nucl. Med. **18**, 432–435 (1991).

[3]A. J. Green, S. E. Dewhurst, R. H. Begent, K. D. Bagshawe, and S. J. Riggs, "Accurate quantification of 131I distribution by gamma camera imaging," Eur. J. Nucl. Med. **16**, 361–365 (1990).

[4]J. A. Sorenson, "Dead time characteristics of anger cameras," J. Nucl. Med. **16**, 284–8 (1975).

[5]J. A. Sorenson, "Methods of correcting anger camera dead time losses," J. Nucl. Med. **17**, 137–41 (1976).

[6]R. Adams, G. J. Hine, and C. D. Zimmerman, "Dead time measurements in scintillation cameras under scatter conditions simulating quantitative nuclear cardiography," J. Nucl. Med. **19**, 538–44 (1978).

[7]R. Wicks and M. Blau "The effect of window fraction on the dead time of anger cameras: Concise communication," J. Nucl. Med. **18**, 732–5 (1977).

[8]J. E. Arnold, A. S. Johnston, and S. M. Pinsky, "The influence of true counting rate and the photopeak fraction of detected events on anger camera dead time," J. Nucl. Med. **15**, 412–6 (1974).

[9]K. Cranley, R. Millar, and T. K. Bell, "Correction for dead time losses in a gamma camera/data analysis system," Eur. J. Nucl. Med. **5**, 377–82 (1980).

[10]M. Ben-Porath, "Camera dead time: Rate-limiting factor in quantitative dynamic studies," Int. J. Nucl. Med. Biol. **2**, 107–12 (1975).

[11]R. Adams, C. Jansen, G. M. Grames, and C. D. Zimmerman, "Dead time of scintillation camera systems—definitions, measurement and applications," Med. Phys. **1**, 198–203 (1974).

[12]R. Adams and I. Mena, "Testing the count rate performance of the scintillation camera by exponential attenuation: Decaying source; multiple filters," Med. Phys. **15**, 415–9 (1988).

[13]M. T. Madsen and R. J. Nickles, "A precise method for correcting count-rate losses in scintillation cameras," Med. Phys. **13**, 344–349 (1986).

[14]A. N. Bice, K. R. Pollard, L. D. Durack, and W. B. Nelp, "Comparative performance of methods for event loss estimation under conditions typical of radioimmunotherapy imaging," J. Nucl. Med. **33**, 1005–1006 (1992).

[15]G. Freeman, T. Kinsela, and A. Dwyer, "A correction method for high-count-rate quantitative radionuclide angiography," Radiology **104**, 713–715 (1972).

[16]G. F. Knoll, *Radiation Detection and Measurement* (Wiley, New York, 1979), p. 99–102.

[17]S. Buchbinder, N. H. Clinthorne, N. Petrick, X. Wang, and K. F. Koral, "A Macintosh-based multienergy data acquisition system for gamma cameras," IEEE Trans. Nucl. Sci. **39**, 864–868 (1992).